BLOOD FLOW AND LIPID TRANSPORT IN A 45 DEGREE BIFURCATION

Nasser Fatouraee[1], Xiaoyan Deng[2], Alain De Champlain[3], and Robert Guidoin[4]

[1]Faculty of Biomedical Engineering, Amirkabir University of Technology (Polytechnic Tehran), Tehran 15914, Iran, [2]College of Biomedical Engineering,The University of Chongqing, Chongqing,400 044,PR China, [3]Mechanical Engineering and [4]Departments of Surgery, Laval University, Quebec, Qc, Canada, G1K 7P4

ABSTRACT

Atherosclerotic lesions may occur in arteries where there are major changes in flow patterns, e.g. bifurcations and junctions. As in an arterial stenosis, disturbed flows in such areas may affect the transport of atherogenic macromolecules and lipids from flowing blood to the luminal surface. The altered transfer of these substances at the junctions, in turn, might result in enhanced lipid infiltration, leading to atherosclerotic lesions. To predict the possible locations of atherogenesis, we used a two-dimensional bifurcation as a human carotid bifurcation model to simulate theoretically the blood flow and to assess quantitatively the effect of a disturbed flow on the luminal surface lipid concentration at the blood/vessel wall interface. The results show that disturbed flows at arterial bifurcations and surgically created junctions enhance atherogenic substance and lipid transfer from flowing blood toward vessel walls. Therefore, these areas have the potential of developing atherosclerotic lesions and are subject to the late failures of grafting resulting from intimal hyperplasia, atherogenic process and anastomotic false aneurysm associated with lipid infiltration.

INTRODUCTION

Although the process involved in the development of atherosclerosis is very complex, histomorphometric examination of early atherosclerotic lesions has demonstrated that the accumulation of cholesterol and other lipids within the intima is an early event in the atherogenic process.[1] A high cholesterol level in the blood is a major risk factor strongly suggesting that the transfer of atherogenic lipids or lipoproteins, especially low density lipoproteins (LDL) from flowing blood to the luminal surface of an artery and their accumulation within the vessel wall, are crucial steps leading to the atherosclerotic changes of arterial wall.[2] In addition, a number of reports have indicated that an abnormal uptake of cholesterol with a high lipid infiltration is the main cause for the late failures of both arterial grafts, biologic[4] and synthetic.[5]

Experimental results by Wiklund *et al.* suggest that the flux of LDL into the arterial wall is not regulated by endothelial LDL receptors. Some cholesterol may seep into the arterial wall by infiltration through leaky endothelial cell junctions. This lipid infiltration should depend on the concentration of lipids at the blood/vessel wall interface which might be much higher than the bulk concentration due to a mass transport phenomenon called concentration polarization. To explore this possibility, we studied numerically the transport of LDL from flowing blood to the arterial wall under both steady-state and pulsatile flow conditions in a straight segment of the human carotid artery[6] and in an arterial stenosis.[7] The numerical analysis predicted that concentration polarization of LDL may occur in the arterial system under both steady-state and pulsatile flow conditions. We believe that the fluid layer with highly concentrated lipids in the region of disturbed flow may increase the driving potential for lipid infiltration into the arterial wall, hence leading to the formation and development of the arterial stenosis.[7]

Arterial bifurcations such as the carotid artery bifurcation are other places in the circulation where the blood flow may be disturbed and a very slow recirculation may occur. Disturbed flows in such areas may also affect the transport of atherogenic macromolecules and lipids from flowing blood to the luminal surface. The altered transfer of these substances at the junctions, in turn, might result in enhanced lipid infiltration, leading to atherosclerotic lesions. To predict the possible locations of atherogenesis, we used a two-dimensional bifurcation as a human carotid bifurcation model to simulate theoretically the blood flow and to assess quantitatively the effect of a disturbed flow on the luminal surface lipid concentration at the blood/vessel wall interface.

Method

Geometric Configurations

The flow geometry is a simplified two-dimensional model of a human carotid bifurcation. The diameter of the main branch (common carotid artery) and the daughter branch were 0.6 cm and 0.4 cm respectively.[8] The bifurcation angle was 45°. The longitudinal and radial coordinates of a point are defined by x, y. These quantities are normalized with respect to the diameter of the common carotid artery, D_C.

Governing Equations

To simplify the analysis, three assumptions were made: (1) The fluid (blood) is homogeneous, incompressible and Newtonian, with a constant viscosity of 0.035 g/cm.sec and a mass density of 1.05 g/cm^3; (2) The vessel wall is permeable to plasma and has a filtration rate on the order of 10^{-6} cm/sec;[9] (3) The convective and diffusive flux of LDL into the vessel wall are so small that their effect on the LDL concentration at the luminal surface is negligible. Based on these assumptions, the blood flow in the bifurcation can be described by the Navier-Stokes equations in the form of the vorticity transport equation. The vorticity η, and the stream function ψ described in two-dimensional coordinates (x,y) were defined by

$$u = \frac{\partial \psi}{\partial x}, \text{ and } v = -\frac{\partial \psi}{\partial y} \tag{1}$$

The only non-zero component of the vorticity is

$$\eta = \frac{\partial v}{\partial x} - \frac{\partial u}{\partial y} \tag{2}$$

and substituting equation (1) gives

$$\nabla^2 \psi = -\eta \tag{3}$$

Taking the curl of the Navier-Stokes equation gives the vorticity transport equation:

$$u \cdot \nabla \eta = \frac{1}{\mathrm{Re}} \nabla^2 \eta \tag{4}$$

where ∇ and ∇^2 are the gradient and Laplacian operators, respectively. Re denotes the Reynolds number and is defined as $\mathrm{Re} = u_0 D_C / \nu$ with u_0 the mean axial velocity in the common carotid artery, D_C the diameter of the common carotid artery and ν is the viscosity of the blood.

Equations (3) and (4) provide the means of determining the flow field in terms of the vorticity and stream function.

The convective and diffusive mass transfer equations in two-dimensional coordinates can be described by

$$u \cdot \nabla c = \frac{1}{\mathrm{ReSc}} \nabla^2 c \tag{5}$$

where u is the velocity vector, c is the normalized concentration and $\mathrm{Sc} = \nu / D$ is the Schmidt number with D as the diffusion coefficient of LDL in blood.

The equations of motion ((3) and (4)) were uncoupled from the mass transfer equation (5), assuming that ν, ρ and D were constants; they could therefore be solved separately.

Boundary Conditions

Flow at the entrance to the common carotid artery was assumed to be Poiseuille flow and the LDL concentration was uniform. At the exits from both the main and the daughter branches, an extrapolated boundary condition was used. With a sufficiently long domain downstream of the flow divider, the flow approaches the fully developed condition and the extrapolation technique used in this study is justified. At the walls the filtration velocity normal to the wall was set constant and the tangential velocity was made equal to zero (no-slip condition). The lipoprotein accumulation at the luminal surface of the artery was determined by imposing a balance between convective and diffusive transports:

$$V_w C_w = \frac{\overline{u}_0 C_0}{\mathrm{ReSc}} \left(\frac{\partial c}{\partial y} \right)_w \tag{6}$$

where C_w denotes the unknown lipoprotein concentration on the luminal surface. This boundary condition is valid for a perfectly rejecting artery, namely, where no lipoproteins pass through the arterial wall (assumption 4).

The flow division ratio between the main and the daughter branches was 70/30 which is based on the average flow ratio in an actual human cardiac cycle.[8]

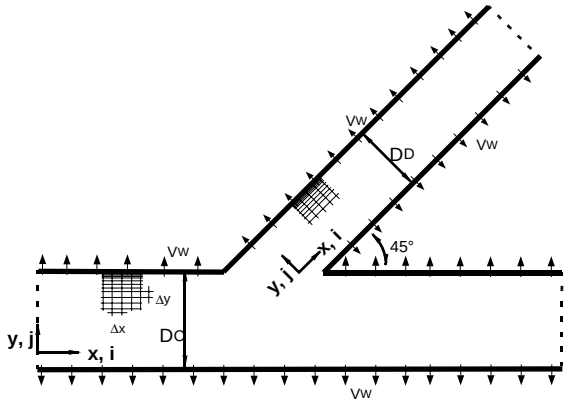

Figure 1. Schematic diagram of the arterial bifurcation with description of the local coordinate systems. The junction has a diameter ratio of 2:3 (daughter branch:main branch).

Numerical Method

To solve the system of equations ((3), (4) and (5)) using finite-difference methods, non-uniform grids were used to minimize the number of nodes while maintaining a sufficient degree of accuracy in the solution. The grid spacing was reduced in the region closest to the vessel wall where high variable gradients and detailed flow parameters are expected. Figure 1 shows a schematic mesh configuration used in this study.

The vorticity-stream function and mass transfer equations ((3), (4) and (5)) in the rectangular computational field were discretized by the central-difference approach. The convective terms of equation (4) were discretized by the second upwind method. For the convective terms in equation (5), a modified upwind method was used.

Results

The calculations were carried out assuming the filtration velocity through the vessel wall to be 1.4×10^{-6} cm/sec which is in the physiological range found in large arteries in humans.[9] At all the Reynolds numbers studied, flow separation occurs in the daughter tube. After the separation point, a triangular shaped vortex forms on the left side of the tube. On the flow divider side, flow remains undisturbed. The length and intensity of the laminar vortex in the daughter vessel increase along with the Reynolds number, and the undisturbed flow zone downstream of the vessel decreases as the vortex widens.

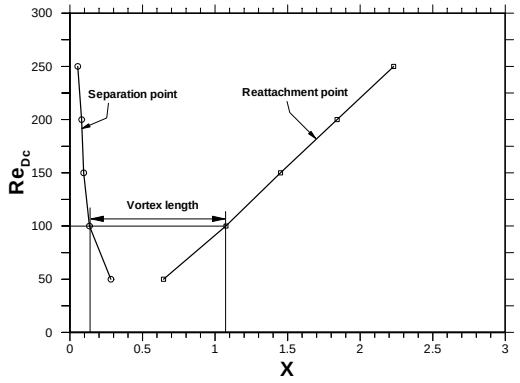

Figure 2. Plot of the flow separation and reattachment points in the daughter branch as a function of Reynolds number, Re. V_W = 1.4 x 10^{-6} cm/sec. Note that for Reynolds numbers less than 50, no recirculation zone formed in the daughter branch.

Figure 2 shows the locations of the flow separation and reattachment points in the daughter branch. Both the locations of flow separation and reattachment points change with the Re. The greater the Re, the closer the separation point to the front corner of the daughter branch. The location of the reattachment points shifts downstream almost linearly with the Re.

The calculation showed that in the main tube, no flow separation appears until the Re reaches 180.

LDL Surface Concentration Distribution

Figure 3 shows a typical flow pattern created in the 2-D bifurcation and the spatial distribution of LDL concentration normalized with respect to the bulk concentration. It is evident here that flow disturbances induced by a flow separation lead to areas of highly concentrated LDL molecules. Most interesting is that the numerical simulation indicates that the weaker vortex zone in the main tube has an higher LDL accumulation at the flow separation point than that in the daughter tube where the vortex intensity is higher.

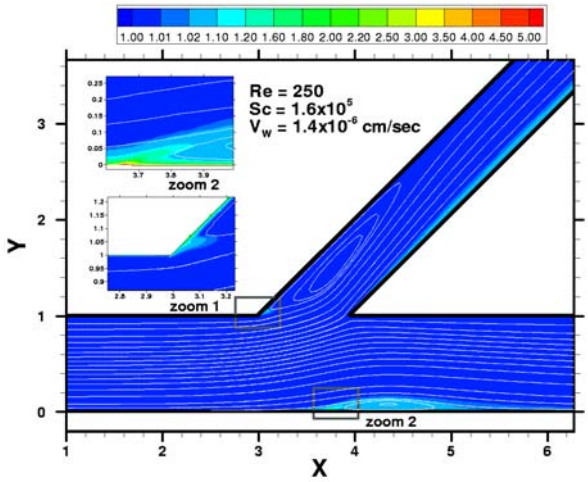

Figure 3. Typical example of streamlines and spatial distribution of normalized LDL concentration with respect to the bulk concentration, C_W/C_0. In the areas of the flow separation points, a highly concentrated LDL fluid layer developed.

Figure 4 shows the distributions of luminal surface LDL concentration along the two parts of the wall junction at four different Re. Along the lower wall (A-B) of the main tube, the steady-state luminal LDL surface concentration in the disturbed flow (Re > 180) is distributed in a totally different fashion than the undisturbed flow (Re < 180). When the Re is less than 180 (undisturbed flow), the luminal LDL surface concentration gradually increases from a constant value upstream to a maximum value at the lowest wall shear rate. Nevertheless, the increase in surface concentration is gradual and smooth. The larger the Re, the higher the maximum value; therefore, the surface concentration of an undisturbed flow situation seems depend on wall shear rate.

On the other hand, when the Re exceeds 180, the luminal surface concentration of LDL in the disturbed flow region is independent of wall shear rate. It increases rapidly in the region of the vortex and reaches a very sharp peak at the flow separation where the wall shear rate is zero. At the flow reattachment point (where the wall shear rate is also zero), no local maximum in luminal LDL surface concentration is predicted. More interestingly, it has been predicted that the peak value for Re = 250 (with flow separation) is lower than that for Re = 150 (without flow separation).

Along the left wall (I-J) in the daughter tube, the theoretical study predicts that the highest accumulation of LDL occurs at the flow separation point. As the Re increases, the peak value of C_w decreases.

Throughout the whole flow field, the theory predicts that when the Re is high enough to create a disturbed flow in the main tube, the highest luminal surface concentration occurs in the main tube (at the flow separation point). However, if the Re is low and no vortex forms in the main tube, the highest surface concentration is in the daughter tube at the flow separation point of the side vortex.

Discussion

The present study found that in the regions of the vortices formed at the junction, the surface concentration of LDL is independent of wall shear rate. Although wall shear rates are zero at both the flow separation and reattachment points, the transport behavior of LDL is very different at these two points. The accumulation of LDL is the highest at the flow separation points of the vortices formed in both the main and the daughter branches. Also, the slower the recirculation flow, the higher the LDL particle accumulation at the luminal surface in the disturbed flow region and the wider the highly concentrated LDL area. This finding qualitatively agrees with the flow observation of Ku *et al*.[10]

Disturbed flows at arterial bifurcations and surgically created junctions enhance atherogenic substance and lipid transfer from flowing blood toward vessel walls. Therefore, these areas have the potential of developing atherosclerotic lesions and are subject to the late failures of grafting resulting from intimal hyperplasia,[11] atherogenic process[12] and anastomotic false aneurysm[5] associated with lipid infiltration.

REFERENCES

1 Stary HC, Arteriosclerosis, 9 (Suppl I): I19-I32, 1989.

2 Page IH, Circulation 10: 1-27, 1954.

3 Debakey ME, Jordan GL, Abbott JP, Halpert B, O'Neal RM, Arch Surg 89: 757-782, 1964.

4 Campeau L, Enjalbert M, Lesperance J, N Engl J Med 311: 1329-1332, 1984.

5 Downs AR, Guzman R, Formichi M, Courbier R, Jausseran JM, Branchereau A, Juhan C, Chakfe N, King M, Guidoin R, Can J Surg 34: 53-58, 1991.

6 Fatouraee N, Deng, XY, De Champlain A, Guidoin R, Ann NY Acad Sci 858: 137-146.

7 Fatouraee N, Deng, XY, De Champlain A, and Guidoin, R, ASME Bioengineering Conference, BigSky, Montana, USA, 1999.

8 Bharadvaj BK, Mabon RF, Giddens DP, J Biomech 15:349-362, 1982.

9 Wilens SL, McCluskey RT: The comparative filtration properties of excised arteries and veins. Am J Med Sci 224: 540-547, 1952.

10 Ku DN, Glagov S, Moore JE, Zarins CK: Flow patterns in the abdominal aorta under simula-ted post prandial and exercise conditions: An experimental study. J Vasc Surg 9: 309-316, 1989.

11 Deweese JA, in Sawyer PN, Kapplitt MJ (eds), Vascular Grafts, New York, Appleton-Century-Crofts, 147-152, 1978.

12 De Palma RG, Atherosclerosis Rev 6: 147-177, 1979.

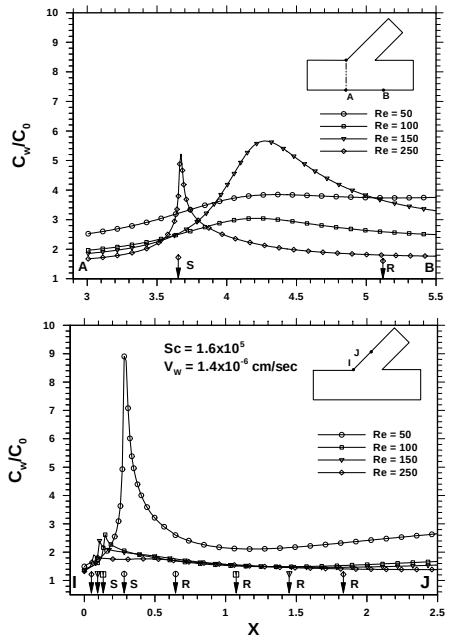

Figure 4. Plots of normalized surface concentration of LDL, Cw/C0, as a function of normalized distance at four different Reynolds numbers, Re. V_W = 1.4 x 10^{-6} cm/sec. The letters S and R indicate the locations of the flow separation point and the reattachment point, respectively.